New Synthesized Guanidine Derivative as a Green Corrosion Inhibitor for Mild Steel in Acidic Solutions

K. F. Khaled[*]

Electrochemistry Laboratory, Chemistry Department, Faculty of Education, Ain Shams University, Roxy, Cairo Egypt
[*]E-mail: khaledrice2003@yahoo.com

A new safe corrosion inhibitor namely N-(5,6-diphenyl-4,5-dihydro-[1,2,4]triazin- 3-yl)-guanidine (NTG) has been synthesized and its inhibitive performance towards the corrosion of mild steel in 1 M hydrochloric acid and 0.5 M sulphuric acid has been investigated. Corrosion inhibition was studied by chemical method (weight loss) and electrochemical techniques include Tafel extrapolation method and electrochemical impedance spectroscopy (EIS). These studies have shown that NTG was a very good inhibitor in acid media and the inhibition efficiency up to 99% and 96% in 1M HCl and 0.5M H_2SO_4, respectively. Polarization measurements reveal that the investigated inhibitor is cathodic in 1M HCl and mixed-type in 0.5M H_2SO_4. Activation energies of the corrosion process in absence and presence of NTG were obtained by measuring the temperature dependence of the corrosion current density. Data obtained from EIS were analyzed to model the corrosion inhibition process through equivalent circuit. Comparable results were obtained by different chemical and electrochemical methods used. The adsorption of the inhibitor on the metal surface in the acid solution was found to obey Langmuir's adsorption isotherm.

1. INTRODUCTION

Corrosion problems have received a considerable amount of attention because of their economic and safety consequences. The use of inhibitors is one of the most practical methods for protection against corrosion. Due to its prominent properties, hydrochloric and sulfuric acids are widely used in industry, for example, acid pickling, industrial acid cleaning, acid descalling and oil-well cleaning. In the previous work, the influence of organic compounds containing nitrogen on the corrosion of mild steel in acidic media have been studied [1-5], Most organic inhibitors act by adsorption on the metal surface [6-9]. It has been known that efficient inhibitors should possess

plentiful of π electrons and unshared electron pairs on nitrogen atoms of the inhibitors which will be given to the vacant *d*-orbital of iron, and by means of transference of electrons, chemical adsorption may occur on the steel surface. Thus, the mild steel corrosion may be suppressed by the protective film on the steel surface.

In continuation of the work on acid corrosion inhibitors [10-12], a new synthesized and safe corrosion inhibitor namely N-(5,6-diphenyl-4,5-dihydro-[1,2,4]triazin-3- yl)-guanidine (NTG) have studied on mild steel in 1 M HCl and 0.5 M H_2SO_4 several chemical and electrochemical techniques have been used to investigate the effect of NTG on corrosion inhibition of mild steel in acidic media

2. EXPERIMENTAL PART

Fig. 1 shows the chemical structure of NTG which obtained by refluxing guanidine hydrochloride with 5,6-diphenyl-4,5-dihydro-[1,2,4]triazine-3-thiol in DMF for 2 hours according to the following reaction:
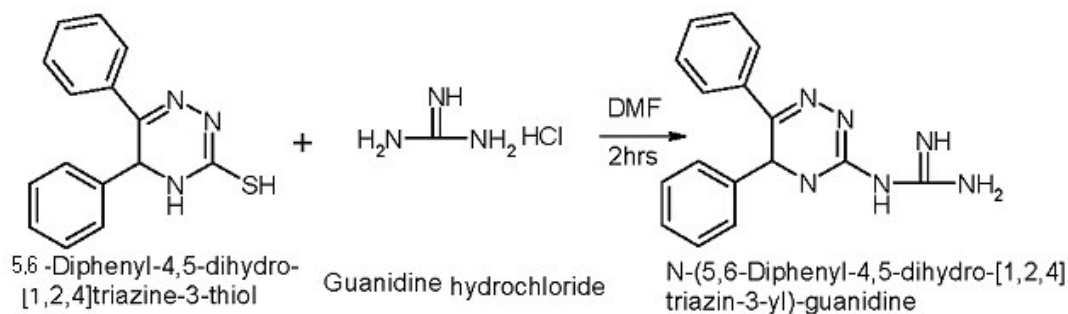
The chemical composition of mild steel rods used in the present work is: C= 0:12%; Mn = 0.85%; S = 0:055%; P = 0.05%; Si = 0.09% and the remainder iron. Steel rods were mounted in Teflon (surface area 0.4 cm^2). The surface preparation of the specimens was carried out using emery papers of different grit sizes up to 4/0 grit and polished with Al_2O_3 (0.5 µm particle size).
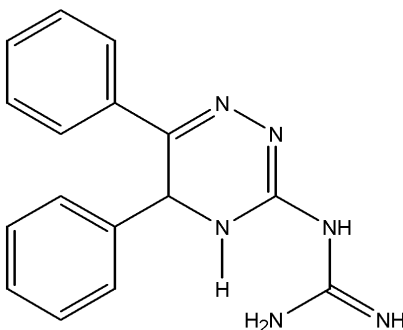
Figure 1. 2D structure of N-(5,6-diphenyl-4,5-dihydro-[1,2,4]triazin-3-yl)-guanidine (NTG)

Weight loss measurements carried out using the mild steel rods, each of size 2 cm length and 0.5 cm diameter (surface area = 6.5 cm^2). The time of immersion was 6 hours and the solution volume was 300 ml. The cleaned samples weighed before and after immersion in acid solutions. The weight loss was expressed in g cm^{-2} h^{-1}.

The electrochemical measurements were performed in a typical three-compartment glass cell consisted of the mild steel rod as working electrode (WE), platinum mesh as counter electrode (CE), and a saturated calomel electrode (SCE) as the reference electrode. The counter electrode was separated from the working electrode compartment by fritted glass. The reference electrode was connected to a Luggin capillary to minimize IR drop. Solutions were prepared from bidistilled water. The electrode potential was allowed to stabilize for 60 min before starting the measurements. All experiments were conducted at 30 ^{o}C. The electrolyte solution was made from analytical reagent grad HCl and H$_2$SO$_4$.

Tafel curves were obtained by changing the electrode potential automatically from (–250 mV$_{SCE}$ to +250 mV$_{SCE}$) versus open circuit potential with scan rate of 0.166mV/s. EIS measurements were carried out in a frequency range of 100 kHz to 50 mHz with amplitude of 10 mV peak-to-peak using ac signals at open circuit potential.

All experiments were carried out in triplicate and the average values were used in corrosion rate calculations.

Measurements were performed with a Gamry Instrument Potentiostat/Galvanostat /ZRA. This includes a Gamry Framework system based on the ESA400 , Gamry applications that include DC105 corrosion and EIS300 electrochemical impedance spectroscopy measurements, along with a computer for collecting the data. Echem Analyst version 4.0 Software was used for plotting, graphing and fitting data.

EIS Spectra analysis was performed using Zview impedance analysis software (Scribner Associates, Inc). For molecular modeling, Hyperchem version 7, a quantum-mechanical program from Hypercube Inc., was used. Molecular orbital calculation was based on semi-empirical Self Consistent Field method (SCF-MO). PM3 semi-empirical SCF- MO method has been used with full optimization of all geometrical variables.

3. RESULTS AND DISCUSSION

3.1. Weight loss measurements

The corrosion parameters such as inhibition efficiency (E%) and corrosion rate ($g.cm^{-2}.h^{-1}$) at different concentration of NTG in 1M HCl and 0.5M H$_2$SO$_4$ at 30 ^{o}C are presented in Table 1. As can be seen in Table 1, NTG inhibits the corrosion of mild steel at all concentrations in both acids. From the determined weight loss values, the inhibition efficiencies, E%, were calculated using the following equation [6]:

$$E\% = (1 - \frac{w}{w_o}) x 100 \qquad\qquad (1)$$

where w_o and w are the weight loss in absence and in the presence of NTG , respectively. Inspection of these data in Table 1, reveals that the inhibition efficiency increases with increasing the concentration of NTG. The corrosion inhibition can be attributed to the adsorption of NTG molecules at mild steel acid solution interface.

Table 1. Corrosion rate and efficiency data obtained from weight loss measurements for mild steel in 1M HCl and 0.5M H_2SO_4 without and with various concentrations NTG.

|	*Inhibitor Conc.* *(M)*	*Corrosion rate* *(g. cm^{-2}.h^{-1})*	*E* *(%)*
	0.0	2.95×10^{-3}	------
	10^{-4}	8.85×10^{-5}	97.0
1M HCl	5×10^{-4}	4.43×10^{-5}	98.5
	$10-3$	2.95×10^{-5}	99.0
	5×10^{-3}	2.36×10^{-5}	99.2
	10^{-2}	1.18×10^{-5}	99.6
	0.0	5.89×10^{-3}	------
	10^{-4}	1.88×10^{-3}	68.0
0.5M H_2SO_4	5×10^{-4}	6.47×10^{-4}	89.0
	$10-3$	4.71×10^{-4}	92.0
	5×10^{-3}	3.59×10^{-4}	93.9
	10^{-2}	5.89×10^{-5}	99.0

3.2. Polarization measurements

Fig. 2 and Fig. 3 depicts typical polarization curves of the mild steel rod in 1M HCl and 0.5M H_2SO_4, in absence and presence of NTG, respectively. As can be seen both anodic and cathodic reactions of mild steel with acids are inhibited as the concentration of NTG increased. NTG inhibits the cathodic reaction greater than the anodic reaction in both acids. Thus, addition of NTG inhibitor reduces the steel dissolution as well as retard the hydrogen evolution reaction. Table 2 shows the electrochemical kinetics parameters, as corrosion potential (E_{corr}), cathodic and anodic Tafel slopes (β_a, β_c) and corrosion current density (i_{corr}), obtained by extrapolation of the Tafel lines. The inhibitor efficiency was evaluated from dc measurements using the following equation [10]:

$$E\% = (1 - \frac{i_{corr}}{i_{corr}^o})x100 \tag{2}$$

where i_{corr}^o and i_{corr} correspond to uninhibited and inhibited current densities, respectively.

Corrosion current density i_{corr} values decreased dramatically by addition of NTG, in both acids. Corrosion potential E_{corr} shifts cathodically in 1M HCl indicating that NTG acts as cathodic type inhibitor in 1M HCl however, there is no definite shift for E_{corr}, in case of NTG in sulphuric acid

indicating that NTG acts as mixed-type inhibitor in 0.5M H_2SO_4. Inhibition efficiency E% increases by increasing concentration of NTG.
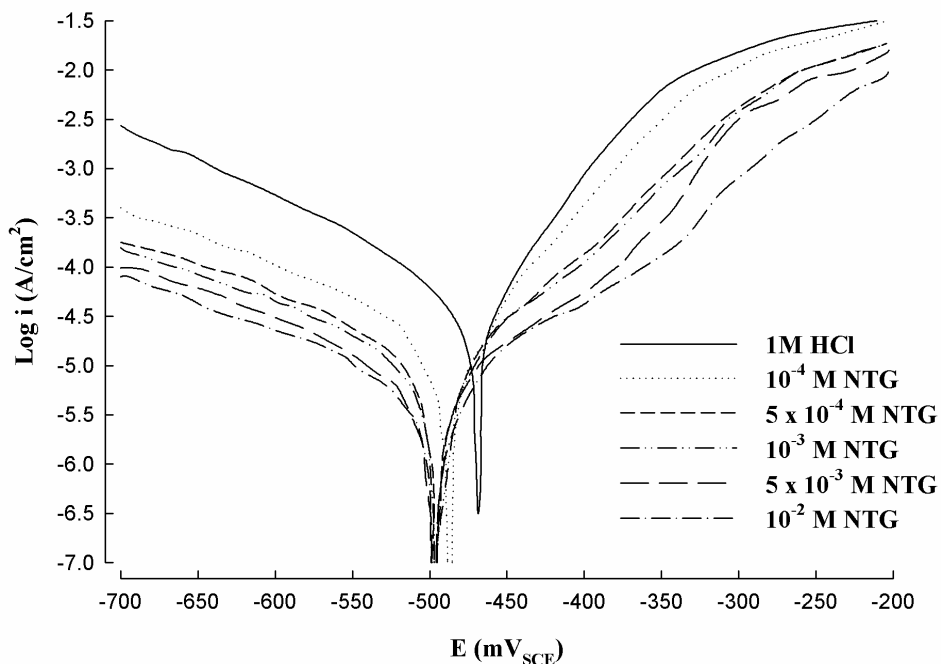
Figure 2. Anodic and cathodic Tafel lines for mild steel in 1M HCl without and with various concentrations of NTG.
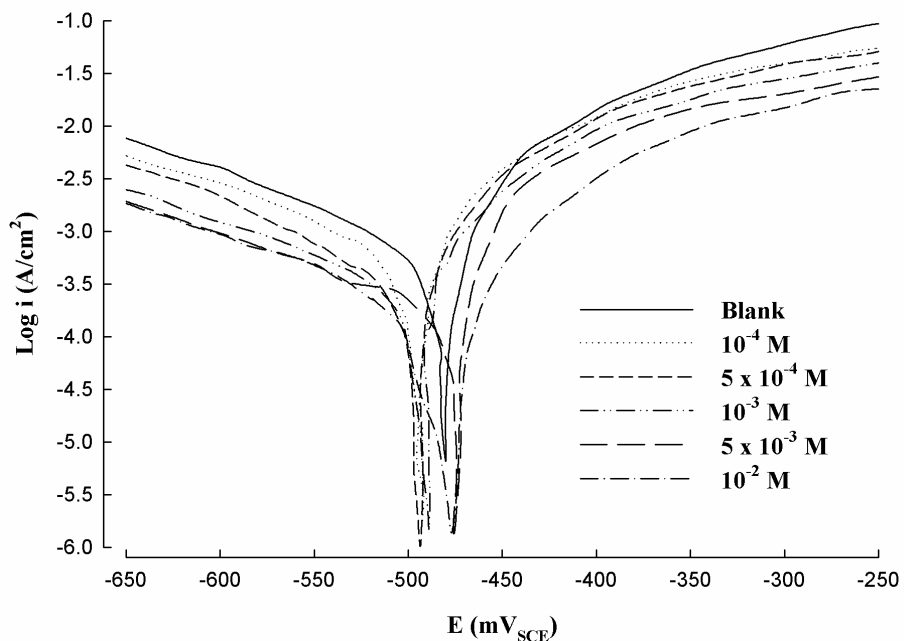
Figure 3. Anodic and cathodic Tafel lines for mild steel in 0.5M H_2SO_4 without and with various concentrations of NTG.

Table 2. Electrochemical kinetic parameters of mild steel in 1M HCl and 0.5M H_2SO_4 without and with various concentrations NTG.

	Conc. *(M)*	i_{corr} *($\mu A.cm_{-2}$)*	*-E_{corr}* *(mV)*	*-β_c* *(mV.dec-1)*	*βa* *(mV.dec-1)*	*C.R* *(mpy)*	*E* *(%)*	Coverage θ
1M HCl	0.0	70.79	470	145	80	32.3	-----	------
	10^{-4}	17.69	490	130	85	12.8	75.01	0.75
	5×10^{-4}	14.86	495	128	85	5.7	79.01	0.79
	10-3	12.03	497	128	86	3.6	83.01	0.88
	5×10^{-3}	6.79	499	125	87	2.8	90.41	0.90
	10^{-2}	4.60	499	123	88	1.8	93.50	0.93
0.5M H_2SO_4	0.0	794.3	480	183	99	362.2	-----	-----
	10^{-4}	413.03	490	172	100	228.2	48.0	0.48
	5×10^{-4}	238.29	495	175	105	181.5	70.0	0.70
	10-3	190.63	490	178	100	144.2	76.0	0.76
	5×10^{-3}	150.92	470	177	102	90.9	80.9	0.90
	10^{-2}	63.54	480	179	100	77.00	92.0	0.92

It has already been observed that the extent of adsorption of the amine is influenced by the nature of anions in acidic solutions [13]. The specific adsorption of anions is expected to be more pronounced with anions having a smaller degree of hydration, such as chloride ions (Cl⁻). Being specifically adsorbed, they create an excess negative charge towards the solution phase, and favor more adsorption of amine cations leading to more adsorption and inhibition of corrosion [14]. Adsorption of organic molecules is not always a direct combination of the organic molecule with the metal surface [15]. In some cases the adsorption occurs through already adsorbed chloride ions in case of HCl or sulphate ions in case of H_2SO_4 that interfere with the adsorbed organic molecules. The lesser interference by sulphate ions may lead to lower adsorption and inhibition of corrosion.

3.3. Effect of temperature on the corrosion inhibition of mild steel

Fig. 4 and Fig.5, show the Tafel plots of mild steel in 1M HCl in absence and presence of 10^{-4} M NTG in temperature range 30-70°C. Effect of temperature has been studied in order to recognize the activation energy of the corrosion process and the thermodynamics of adsorption of NTG on mild steel surface. Data in Table 3 shows that by increasing the temperature the corrosion rate increases in absence and presence of NTG. Also, the corrosion rate increases rapidly in absence of NTG , on addition of NTG, the corrosion rate rapidly decrease i.e. NTG is an efficient inhibitor in the temperature range 30-70°C and the values of inhibition efficiency is almost constant in the temperature range 50-70°C.

The activation parameters are calculated from Arrhenius-type plot according to equation [9]:

$$\ln i_{corr} = -\frac{E_a}{RT} + A \qquad (3)$$

E_a is the apparent activation energy, R is the ideal gas constant. A plot of ln i_{corr} vs. $1/T$ gives a straight line with slope of $-E_a/R$. The values of activation energies are calculated from the slopes of Arrhenius plots, Fig.6. By addition of NTG, the activation energy reduced from 106.23 to 41.98 KJmol^{-1} which may be attributed to the chemisorption of NTG on mild steel surface [16-17].With increasing the temperature, some chemical changes occur in the inhibitor molecules, leading to an increase in the electron densities at the adsorption centers of the molecule, causing an improvement in inhibitor efficiency [18].
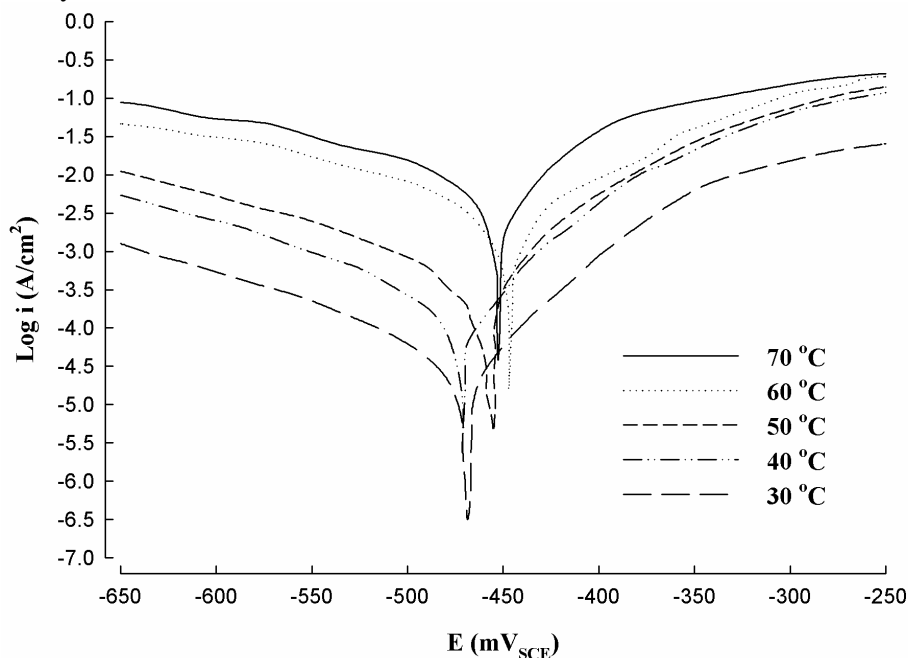

Figure 4. Anodic and cathodic Tafel lines for mild steel in 1M HCl at temperature range (30-70)^{o}C.
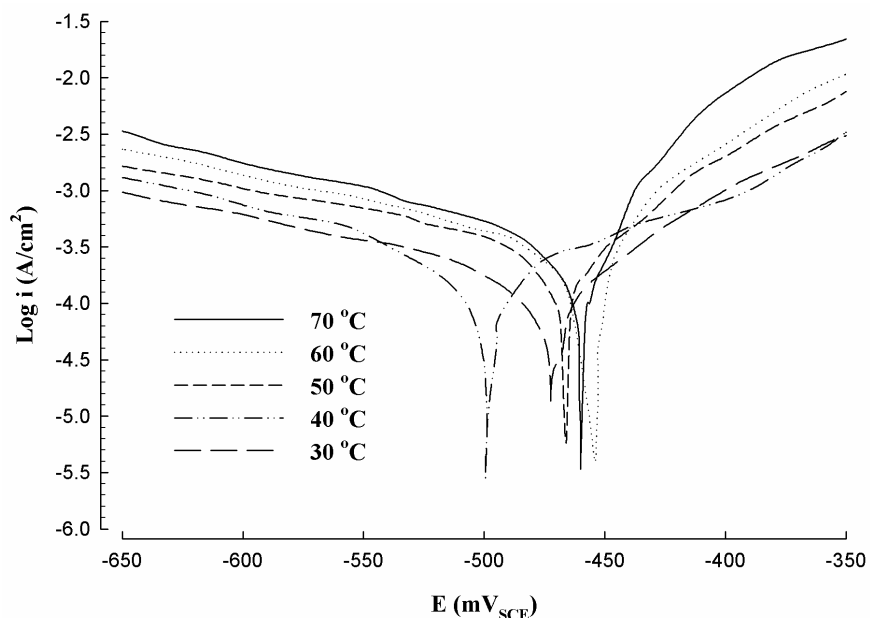
Figure 5. Anodic and cathodic Tafel lines for mild steel in 1M HCl with 10^{-4} M NTG at temperature range (30-70)^{o}C.

Table 3. Electrochemical kinetic parameters of mild steel in 1M HCl without and with 10^{-4} M NTG at temperature range 30-70 ^{o}C.

|	*Temp.* ^{o}C	i$_{corr}$ ($\mu A.cm_{-2}$)	-E$_{corr}$ (mV)	-β_c (mV.dec$_{-1}$)	βa (mV.dec$_{-1}$)	C.R (mpy)	E (%)
1M HCl	30	70.79	470	145	80	32.3	
	40	398.1	480	130	85	181.5	
	50	3715.3	447	128	85	1694.2	
	60	6039.4	455	128	86	2753.9	
	70	7943.2	450	125	87	3622.1	
1M HCl + NTG	30	17.69	490	183	99	8.07	75.01
	40	50.12	500	172	100	22.8	87.4
	50	63.1	480	175	105	28.7	98.3
	60	79.4	460	178	100	36.2	98.6
	70	158.0	470	177	102	72.1	98.1
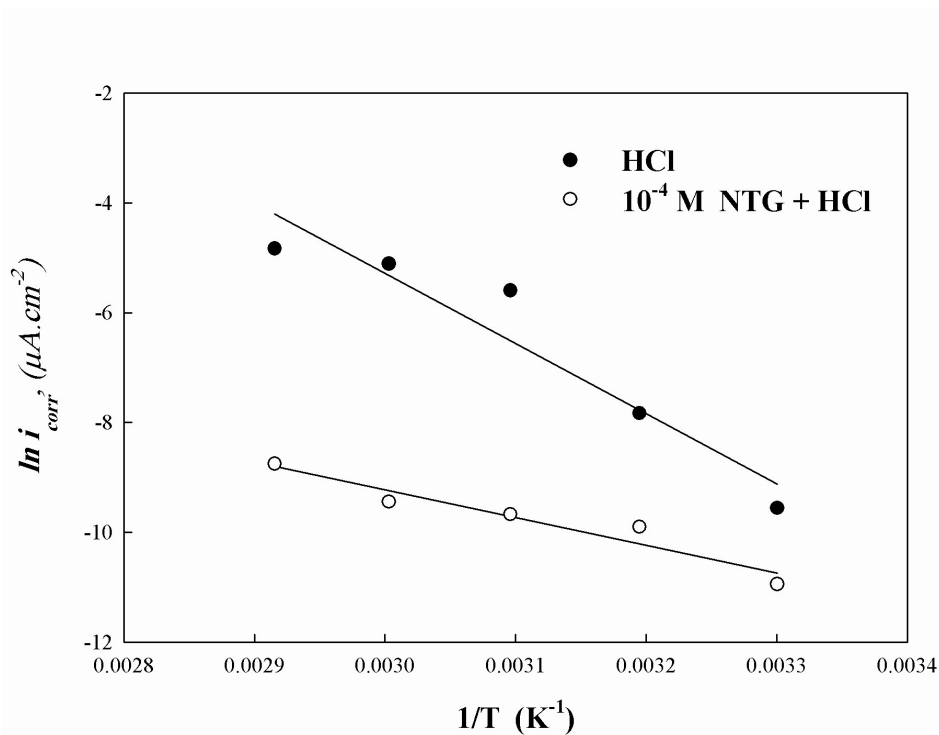
Figure 6. Arrhenius plots of the corrosion rate of mild steel in 1M HCl and 1M HCl +10^{-4}M NTG.

3.4. Electrochemical impedance measurements

The corrosion behaviour of mild steel in both acids in absence and presence of NTG investigated by EIS at 30°C. Nyquist plots of mild steel in uninhibited and inhibited acidic solutions containing various concentrations of NTG are presented in Fig. 7 and Fig.8. It is obvious from these plots that the impedance response of mild steel has significantly changed after addition of NTG. It is clear that the shapes of the impedance plots for inhibited electrodes are not substantially different from

those of uninhibited electrodes. The presence of the inhibitor increases the impedance but does not change other aspects of the behaviour. These results support the results of polarization measurements that the inhibitor does not alter the electrochemical reactions responsible for corrosion. It inhibits corrosion primarily through its adsorption on the metal surface.
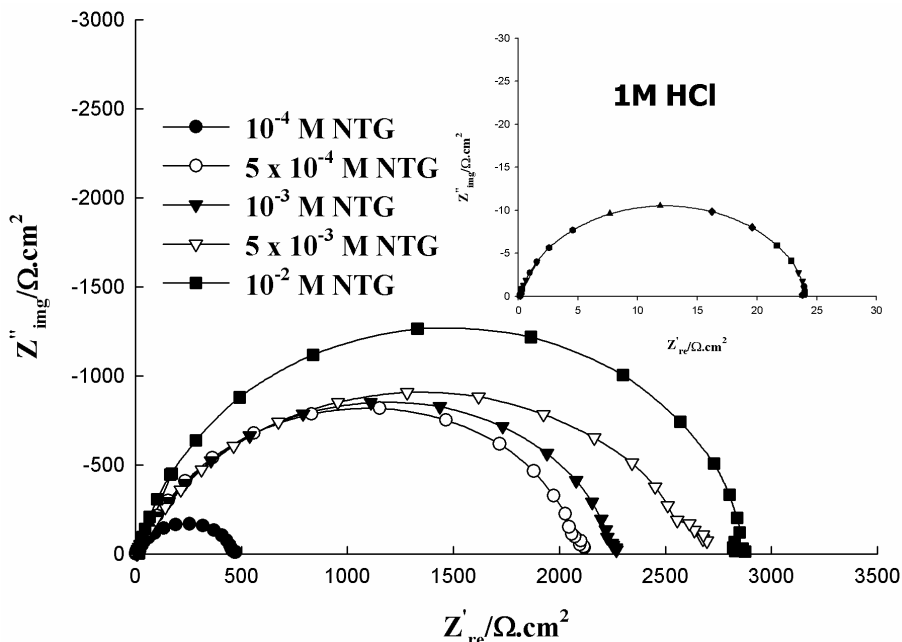

Figure 7. Complex-plane impedance for mild steel in 1M HCl without and with various concentrations of NTG symbols refer to experimental data and solid lines to fitted data.
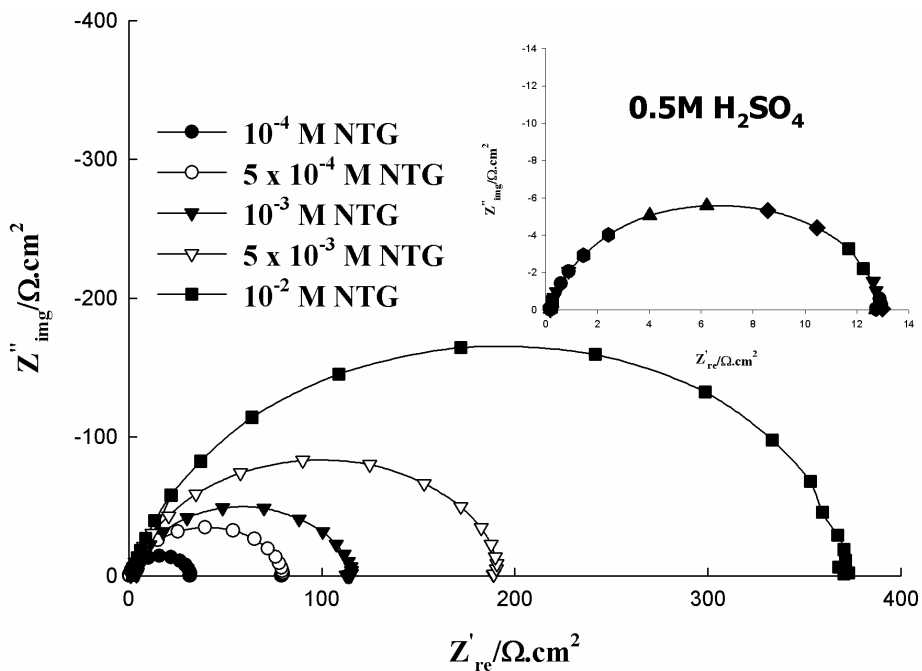
Figure 8. Complex-plane impedance for mild steel in 0.5M H_2SO_4 without and with various concentrations of NTG symbols refer to experimental data and solid lines to fitted data.

To determine the impedance parameters of the mild steel specimens in acidic solutions, the measured impedance data were analyzed by using Zview impedance analysis software (Scribner Associates, Inc) , based upon the electric equivalent circuit given in Fig. 9. The equivalent circuit consists of Constant Phase Element (CPE) in parallel with polarization resistance R_p which is in series with solution resistance R_s values of these components and inhibition efficiencies are derived from EIS measurements and presented in Table 4. It is clear from Table 4 that the impedance of the inhibited system increased with increasing the inhibitor concentration and the CPE values decrease with increasing NTG concentration.
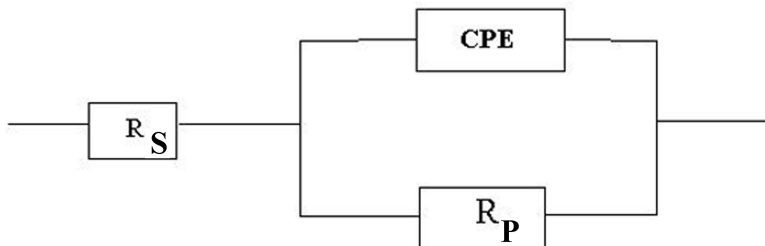
Figure 9. Equivalent circuit model for NTG, R_s solution resistance, R_p polarization resistance and CPE constant phase element.

Table 4. Impedance data of mild steel in 1M HCl and 0.5M H_2SO_4 without and with various concentrations NTG obtained from analysis of NTG according to equivalent circuit at Fig. 9.

	Inhibitor Conc. (M)	R_s $(\Omega.cm^2)$	R_{ct} $(\Omega.cm^2)$	*CPE* (μFcm^2)	*n*	*E (%)*
	0.0	0.8	24.00	24.5	0.89	------
	10^{-4}	1.3	470	22.15	0.78	94.8
1M HCl	5×10^{-4}	2.3	2143	21.91	0.80	98.8
	10^{-3}	2.2	2302	18.6	0.79	98.9
	5×10^{-3}	2.1	2630	10.5	0.77	99.1
	10^{-2}	1.1	2872	6.2	0.80	99.2
	0.0	0.18	12.87	71.92	0.89	------
	10^{-4}	1.2	32.33	59.52	0.87	60.2
0.5M H_2SO_4	5×10^{-4}	2.5	79.7	47.68	0.89	83.8
	10^{-3}	2.8	115.7	46.31	0.89	88.8
	5×10^{-3}	2.7	192.5	38.35	0.88	93.3
	10^{-2}	2.6	375.1	35.86	0.89	96.5

One constant phase element (CPE) is substituted for the capacitive element C_{dl} , double layer capacitance to give a more accurate fit [19], as the obtained capacitive loop is a depressed semi-circle rather than regular one. The CPE is a special element whose immittance value is a function of the angular frequency (ω), and whose phase is independent of the frequency. Its admittance and impedance are, respectively, expressed as:

$$Y_{CPE} = Y_0 \, (j\omega)^n \tag{4}$$

and

$$Z_{CPE} = (1/Y_0) \, [(j\omega)^n]^{-1} \tag{5}$$

where Y_0 is the magnitude of the CPE, j is the imaginary number ($j^2 = -1$), α is the phase angle of the CPE and $n = \alpha/(\pi/2)$. The factor n is an adjustable parameter that usually lies between 0.50 and 1.0 [20]. Values of the parameter n are presented in Table 4. The CPE describes an ideal capacitor when n = 1. Values of α are usually related to the roughness of the electrode surface. The smaller value of α, the higher the surface roughness [20,21]. A good fit with this model was obtained with our experimental data. It is observed that the fitted data match the experimental, with an average error of about 2%. The symbols in Figs. 7 and 8 represent the experimental data, while the solid lines represent the best fits.

This decrease in CPE / C_{dl} results from a decrease in local dielectric constant and /or an increase in the thickness of the double layer, suggested that NTG molecules inhibit the steel corrosion by adsorption at the metal/acid interface [22]. Similar behaviour was observed in both HCl and H_2SO_4 acids as well as in our previous study [23]. These plots have the appearance of a semicircle corresponding to a charge transfer controlled process.

The more densely packed the monolayer of NTG, the larger the diameter of the semicircle, which results in higher R_p and lower CPE / C_{dl} values.

The impedance spectra obtained for mild steel in both acid media contains depressed semicircle with the center under the real axis, such behavior is characteristic for solid electrodes and often referred to as frequency dispersion and attributed to the roughness and other inhomogenities of the solid electrode [24-25].

By comparing the values of inhibition efficiencies obtained from both EIS and weight loss methods with those obtained from Tafel extrapolation method , it is observed that, there is no agreement between these values. This observation was reported by several authors [26-28]. Corrosion rate obtained by polarization is one application of perturbation technique. It is quite different from the rate obtained by weight loss method and EIS which is not perturbing the electrode [29]. This observation was also reported by several authors [27-30] and they attribute this difference between electrochemically and chemically determined rates to the operation of a separate potential independent of chemical dissolution process which co-exists with the electrochemical process but not by the polarization curve [30].

3.5. Adsorption isotherm

In order to gain more information about the mode of adsorption of NTG on the surface of mild steel at different temperatures, the experimental data have been tested with several adsorption isotherms. In order to obtain the isotherm, coverage θ as a function of NTG concentration must be obtained. Coverage can be obtained from polarization measurement by the following equation [31]:

$$\theta = 1 - \frac{i_{corr}}{i^o_{corr}} \qquad (6)$$

where i^o_{corr} and i_{corr} correspond to uninhibited and inhibited current densities, respectively. The best fit was obtained with Langumir adsorption isotherm as in Fig. 10. According to Langumir isotherm, Coverage θ is related to inhibitor concentration C_{inh} by the following relation [31]:

$$\theta = \frac{bC_{inh}}{1 + bC_{inh}} \qquad (7)$$

where b is the adsorption coefficient. The value of b has been calculated from the Langumir adsorption isotherm in 1M HCl and 0.5M H_2SO_4 and found to be 12306.63 M^{-1} and 5659.3 M^{-1}, respectively. The high value of b in the case of 1M HCl indicated that NTG was strongly adsorbed on the steel surface [32]. Adsorption of NTG on mild steel surfaces can be achieved by two modes of adsorption, through the free lone pairs on nitrogen atoms as well as π-electrons of the phenyl rings and protonated species of NTG as they are present in acidic media, nitrogen atoms accept protons from the acid solution and form cations which electrostatically attracted to the pre-adsorbed Cl^{-1} or SO_4^{-2} anions on the mild steel surfaces.
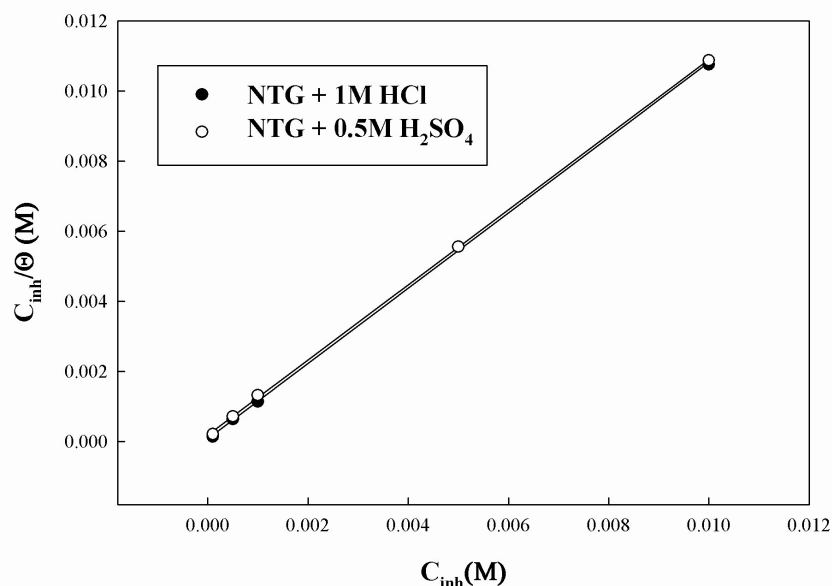
Figure 10. Langmuir adsorption plots of mild steel in 1M HCl and 0.5M H_2SO_4 containing various concentrations from NTG at 30 °C.

Relationship between electronic structures of NTG was deducted from quantum chemical indices E_{HOMO} (-9.1 eV), E_{LUMO} (-0.78 eV), E_{HOMO}-E_{LUMO} (-8.22 eV) and dipole moment μ (6.1D) of NTG. The high inhibition efficiency of NTG can be attributed to the high value of E_{HOMO} and dipole moment μ and low value of E_{LUMO}. The results seem to indicate, that charge transfer from NTG takes place during adsorption to the steel surface. High value of E_{HOMO} may facilitate adsorption (and therefore inhibition) by influencing the transport process through the adsorbed layer [33].

4. CONCLUSIONS

In this study, it was shown that N-(5,6-diphenyl-4,5-dihydro-[1,2,4]triazin-3- yl)-guanidine (NTG), is effective inhibitor of corrosion of mild steel exposed to 1M HCl and 0.5M H_2SO_4. NTG has better performance in 1M HCl than 0.5M H_2SO_4.

Polarization data shows that NTG acts as cathodic inhibitor in 1M HCl and mixed-type inhibitor in H_2SO_4. In temperature range 50-70°C, the inhibition efficiency of NTG is temperature-independent and the addition of NTG decreases the activation energy. In determining the corrosion rate, electrochemical studies and weight loss measurements give comparable results. There are differences between the efficiencies obtained from Tafel polarization technique and both EIS and weight loss methods. This difference in determined corrosion rates is due to the operation of a separate potential independent of chemical dissolution process which co-exists with the electrochemical process but not by the polarization curve.

NTG is adsorbed on the steel surface through free electron pairs on the nitrogen atoms as well as π-electrons of the phenyl rings that can interact with the vacant *d-orbital* of iron, and in the form of protonated species with already adsorbed anions (Cl^{-1} or SO_4^{-2}).

References

1. N. Ochoa, F. Moran, N. Pébère and B. Tribollet, *Corros. Sci.*, 47 (2005)593.
2. P. Ocón, A.B. Cristobal, P. Herrasti and E. Fatas, *Corros. Sci.*, 47 (2005)649.
3. E.A. Noor, *Corros. Sci.*, 47 (2005) 33.
4. A. Frignani, C. Monticelli, F. Zucchi and G. Trabanelli, *Mater. Chem. & phys.*92 (2005) 403.
5. M. Karakuş, M. Şahin and S. Bilgiç, *Mater. Chem.& phys.* 92 (2005) 565.
6. S. S. Abdel Rehim, Magdy A. M. Ibrahim and K. F. Khaled „*J. Appl. Electrochem.*, 29 (1999) 597.
7. K. F. Khaled, S. S. Abdel Rehim and N. Hackerman, *Ann. Univ. Ferrara*, 2 (2000) 713.
8. K. Babic-Samardzija , K. F. Khaled and N. Hackerman *Anti corros. Meth. and Mater.* 52 (2005)11.
9. S. S. Abdel Rehim, Magdy A. M. Ibrahim and K. F. Khaled , *J. corros. prevent. & contr.*, 3 (2000) 245.
10. S. S. Abdel Rehim, Magdy A. M. Ibrahim and K. F. Khaed , *J. Mater. Chem. & Phys.*, 70 (2001) 267.
11. K. F. Khaled, *Electrochim. Acta*, 48 (2003) 2493.
12. K. F. Khaled and N. Hackerman, *Electrochim. Acta* ,48 (2003) 2715.
13. Z. A. Foroulis, Proc. 6th European Symposium on corrosion Inhibitors, *Ann. Univ. Ferrara, Italy*, N.S., sez. V, Suppl. N. 8 (1985)130.
14. Z. A. Iofa and G.N. Tomashov, *Zh. Fiz. Khim.* 34 (1960) 1036.
15. T. Murakawa and N. Hackerman, *Corros. Sci.* 4 (1964) 387.
16. T. Szauer and A. Brand, *Electrochim. Acta* 26 (1981)1219.
17. S. Muralidharan, F. Pushpanaden and M. Ahmed, *Corros. Sci.* 32 (1991) 193.
18. D.D.N. Singh, R.S. Chaudhary, B. Prakash and C. V. Agarwal, *Br. Corros. J.* 14 (1979) 235.

19. J.R. Macdonald, Impedance Spectroscopy, Wiley, New York (1987).
20. B.A. Boukamamp, *Solid State Ionics* 20 (1980) 31.
21. A.V. Benedetti, P.T.A. Sumodjo, K. Nobe, P.L. Cabot and W.G. Proud, *Electrochim. Acta* 40 (1995), p. 2657.
22. M.Lagrenee, B. Mernari, M. Bouanis, M. Traisnel, *Corros. Sci.* 44 (2002) 573.
23. K.F.Khaled, *Appl. Surf. Sci.,* 252, (2006) 4120
24. K. Juttner, *Electrochim. Acta* 35 (1990) 1501.
25. T.Pajkossy, *J. Electroanal.chem.* 364 (1994) 111.
26. N. Hackerman, R.M. Hurd, R.R. Annand, *Corrosion* 18 (1962) 37.
27. G. Oskes, J.M. West, *Br. Corrosion J.* 4 (1969) 6617.
28. G.M. Florianovich, M. Kolotyrkin, I.A. Sokolova, 3rd International Conference on Metallic Corrosion Moscow, 1, 1966, p. 192.
29. E.E.F. El Sherbini, *J. Material Chem. & Phys*., 61 (1999) 223
30. E.E.F. El Sherbini, S. M. Abd-El-Wahab and M. A. Deyab, *J. Material Chem. & Phys*., 82 (2003) 631.
31. N. Hackerman and E. McCafferty, Proceeding of the fifth International Congress on Mettalic Corrosion, Tokyo, (1972) 542.
32. J.D.Talati and D. K. Gandhi, *Corros. Sci*. 23 (1983) 1315.
33. I. Lukovits, E. Kalman, I. Bako, I. Felhosi and J. Telegdi, Proc. Eighth European Symposium on Corrosion inhibitors, Ann. Univ. Ferrara, N. S., Sez. V, Suppl. N. 10 (1995) 543.